NEW RESULTS ON JET FRAGMENTATION AT THE CERN SPS COLLIDER

UA1 Collaboration, CERN, Geneva, Switzerland

Aachen-Amsterdam (NIKHEF)-Annecy (LAPP)-Birmingham-CERN-Harvard-Helsinki-Kiel-London (Queen Mary College)-Padua-Paris (Coll. de France)-Riverside-Rome-Rutherford Appleton Lab.-Saclay (CEN)-Vienna-Wisconsin

Presented by P. Ghez, Annecy (LAPP), France

ABSTRACT

We report new results of jet fragmentation into charged tracks in the UA1 experiment. A new estimate of the fragmentation function shows strong differences between our data and those of PETRA. A preliminary analysis suggests a different quark and gluon fragmentation which is well reproduced by a recent model. The observed scaling violations of the fragmentation function and of the internal p_T are consistent with QCD expectations.

1. INTRODUCTION

The intensive production of large-p_T jets in hadron-hadron collisions at very high energy is taken as evidence for quark and gluon hard collisions[1]. This production is understood as the result of parton-parton scattering followed by fragmentation of scattered partons in hadrons. Such events show a dominant two-jet (large p_T) structure, with occasional further jets due to gluon bremsstrahlung. At the CERN Super Proton Synchrotron (SPS) Collider one can expect these jets to come primarily from a $gg \to gg$ subprocess[2]; quark jets coming from a $qg \to qg$ subprocess may also be present.

In this paper we will show results on inclusive fragmentation properties of jets (mostly gluon jets) based on a very large sample. We will also give results of a preliminary attempt to observe fragmentation differences between quark and gluon jets. The basic assumptions for this analysis are the following:

- in order to get the cleanest possible sample (not being limited by statistics), we have restricted our study to clean two-jet events;
- we have assumed, in all that follows, that the fragmentation of a given jet can be considered independently of the other jet (Independent Fragmentation).

2. DATA SAMPLE AND DEFINITIONS

2.1 Data Sample

The data sample comes from the full sample of the 1983 data-taking period at $\sqrt{s}$ = 546 GeV. An 'inclusive jet' trigger was selected for a total luminosity of ~ 110 events per nanobarn. The events were fully processed and the jets were obtained with the UA1 jet algorithm[3]. This procedure, applied on calorimeter cells, determined the energy/momentum (E/p), the pseudorapidity (η), and the azimuth (φ) of each jet.

We have selected the two-jet topology by imposing a minimum E_T (25 GeV) on the leading jet of each event, and by requiring that the two jets are back-to-back (within 30°) in the transverse plane.

We have required each individual jet to be in a good acceptance region both for the calorimetry and for the central detector (CD). Another requirement was that each jet responsible for the hardware trigger ('triggering jet') be sufficiently high above threshold to avoid any trigger bias.

Our cleaned sample contains ~ 15,000 jets with

$$\begin{cases} E_T > 15 \text{ GeV}, & \\ |\eta| < 1.4, \quad 30^\circ < \varphi < 60^\circ & (+\, n\pi/2), \\ 1.7 < |\eta| < 2.5, \quad 0^\circ < \varphi < 60^\circ & (+\, n\pi/2), \end{cases}$$

2.2 Definitions

The charged tracks are associated with the jets in the following way: for a given jet, one includes all tracks having $\Delta R < 1$, where $\Delta R = \sqrt{(\eta_{jet}-\eta_{track})^2 + (\varphi_{jet}-\varphi_{track})^2}$ for tracks of $z > 0.01$; z is defined as p_L^{track}/p_{jet} (p_L^{track} is the projection of the track momentum on the jet axis; p_{jet} is the modulus of the vector sum of the energy vectors associated with the calorimeter cells contained in the jet).

The internal transverse momentum p_T^{track} is simply the track transverse momentum with respect to the jet axis, determined in this case (for more precision) from charged tracks only.

3. RESULTS ON INCLUSIVE PROPERTIES

3.1 Fragmentation Function: F(z)

The fragmentation function is defined as $F(z) = (1/N_{jet})(dN_{ch}/dz)$. Several corrections have to be applied to the raw fragmentation function:

- Subtraction of tracks coming from the rest of the event ('background' tracks). This causes a depletion of F(z) at very low z ($z < 0.05$).
- Acceptance correction due to track losses near the horizontal plane ($\vec{B}$ and drift wires are both horizontal). This correction is z invariant and causes a rescaling of F(z) of the order of ~ 20%.
- Jet energy correction. The limited aperture of the $\Delta R < 1$ cone (used also to determine the jet energy), detector inefficiencies, and the fluctuations of the calorimeter response with the jet content cause a loss of jet energy. On the other hand, the rest of the event causes a gain of energy in the measurement of the jet energy. These effects have been extensively studied with Monte Carlo events, and correction tables have been obtained[4]. Applying these energy corrections produces a rescaling of the z axis, and the resulting changes (depletion at large z) are far from negligible.
- The smearing effect due to the track momentum and jet energy errors has been corrected for. The method (cross-checked with simulated events) involves a limited expansion of the smearing integral, from which one gets a correction factor depending on the track momentum error (for each track) and on the jet momentum error (for each jet).

The last two corrections were underestimated in our preceding publication[5] on this topic and are responsible for the changes observed in the fragmentation function. The correction procedure involves large correction factors, and we have checked their validity with simulated data where all details of the apparatus were reproduced.

The fully corrected F(z) is shown in Fig. 1 together with (properly renormalized) PETRA results[6] and also with a preliminary prediction using a parton-parton showering scheme and the LUND hadronization[7]. The systematic errors are essentially dominated (at low z) by the background estimation and (at high z) by the jet energy correction. Our data fit well the following empirical function: $F(z) = (3.6/z)e^{-8z}$. This result is not compatible with PETRA results. This incompatibility can be due to the Q^2 evolution of F(z), to the nature (gluon) of the fragmenting parton, and possibly to the different nature of the hard collision (hadron-hadron versus lepton-lepton). However, the comparison of our data with a very recent model based on parton shower evolution (for the perturbative part of the fragmentation) and the LUND prescription (for the non-perturbative part: hadronization) is satisfactory (see Fig. 1).

3.2 Internal Transverse Momentum within the Jet

It has already been pointed out that the very low momentum tracks are difficult to associate[5] with the jet; therefore in defining $\langle p_T \rangle$ we have applied a cut on the minimum longitudinal momentum: $z > 0.1$ to accept a track. This cut, owing to the known 'seagull' effect, is responsible for an artificially high value of $\langle p_T \rangle$. This cut removes all the background and acceptance effects. Starting from the raw distribution, we are left with only one correction to be applied to the data: the unsmearing of the track momentum error, which has been computed as for the fragmentation function.

Figure 2 shows the corrected invariant p_T spectrum:

$$\frac{1}{N_{jet}} \quad \frac{1}{p_T} \quad \frac{dN_{ch}}{dp_T}$$

together with a preliminary prediction of the model already described[7]. We observe an exponential decrease of the p_T, giving a mean value:

$$\langle p_T \rangle \sim 850 \text{ MeV} \qquad (\text{for } z > 0.1).$$

4. QUARK AND GLUON FRAGMENTATION -- METHOD

We have adopted the following method to distinguish between quark and gluon jets:

- Since each two-jet event (p_T, η_1, η_2) defines unambiguously the parton-parton kinematics with the variables (x_1, x_2, $\cos\theta^*$) where x_1 (x_2) are the p ($\bar{p}$) momentum fractions of the interacting partons, and $\cos\theta^*$ is the scattering angle in the parton-parton c.m.s., one can compute the cross-section of each subprocess, which is proportional to

$$F_p(x_1, Q^2)\ F_{\bar{p}}(x_2, Q^2)\ \frac{d\hat{\sigma}}{d\hat{t}}\ (\hat{s}, \hat{t}, \hat{u}),$$

  where

  F_p, $F_{\bar{p}}$ are the structure functions;
  $d\hat{\sigma}/d\hat{t}$ is the parton-parton elastic cross-section;
  $\hat{s}$, $\hat{t}$, $\hat{u}$ are the Mandelstam variables of the subprocess (connected to $\cos\theta^*$).

- We have computed each subprocess cross-section assuming:
  a) the parametrization of the structure functions from Ref. 8;
  b) the standard first-order QCD matrix element for the parton-parton elastic scattering[9];
  c) $Q^2 = 2\ \hat{s}\ \hat{t}\ \hat{u}/(\hat{s}^2 + \hat{t}^2 + \hat{u}^2)$.

For each jet, we can calculate the probability for this jet to be a gluon by summing all relevant subprocess cross-sections:

$$P(\text{jet} = \text{gluon}) = \frac{\sum_{\text{process}}(\text{jet} = \text{gluon})}{\sum_{\text{process}}(\text{jet} = \text{anything})},$$

and of course: $P(\text{jet} = \text{quark}) = 1 - P(\text{jet} = \text{gluon})$.

Figure 3 shows the histogram of this probability. We observe that, if gluon jets dominate, some quark jets seem to be present.

The kinematical calculations are defined as in Ref. 10, but the results are not sensitive to this specific choice. Also, the results are not too sensitive to

- the choice of the structure function parametrization,
- the definition of Q^2.

To separate gluon and quark jets, we have chosen two separate bins:

$0.5 < P(\text{jet} = \text{gluon}) < 0.7 \qquad \langle P \rangle = 0.6$: 'gluon'

$0.1 < P(\text{jet} = \text{gluon}) < 0.3 \qquad \langle P \rangle = 0.2$: 'quark'

and when plotting the gluon/quark distributions we have solved a system of linear equations to get 'pure' samples.

5. QUARK AND GLUON FRAGMENTATION -- RESULTS

5.1 Fragmentation Function

The ratio between gluon and quark fragmentation functions for 'pure' samples is shown in Fig. 4 together with a preliminary prediction[7]. The dominance of gluon jets at low z (larger multiplicity) is visible, whereas at high z, the situation dominated by our large systematic errors is less clear.

The Q^2 evolution for each sample is shown in Figs. 5 (gluon) and 6 (quark). The observed behaviour follows the QCD expectations:

- the longitudinal fragmentation is softer when Q^2 increases, in both samples;
- this scaling violation effect seems weaker for quark jets than for gluon jets.

5.2 Internal Transverse Momentum within the Jet

Figure 7 shows the ratio of the p_T distributions between 'pure' samples of gluon and quark jets. The observed differences are very significant in this variable because of lower systematic errors. We observe the following behaviours:

- Gluon jets are broader than quark jets.
  The fit to an exponential of the two separated distributions gives: $\langle p_T \rangle_g \sim 900$ GeV, $\langle p_T \rangle_q \sim 800$ GeV.
- The agreement with the model[7] is very good.

The Q^2 evolution for the non-pure (enriched) samples is shown in

Figs. 8 (gluon) and 9 (quark). Again the Q^2 evolution of the internal p_T is similar to the one observed for the fragmentation function:
- broadening of the jet with increasing Q^2;
- weaker broadening for quark jets than for gluon jets.

5.3 Jet Charge

We have determined the charge of each jet using different definitions as proposed by Field and Feynman[11]:

1) Jet charge = charge of the leading particle
2) Jet charge = charge of the leading + next-to-leading particle
3) Jet charge = $\sum_i Q_i z_i^{0.3}$ (i = all associated tracks).

These three different definitions give similar results; we give a summary of these results in the table (the results of the three methods are within the error bars):

		P(jet = gluon) > 70%	P(jet = u quark) > 70%	P(jet = $\bar{u}$ quark) > 70%
Charge (%)		-1.6 ± 2.5	+19.6 ± 3.3	-23.6 ± 3.8
Pure sample	Ref. 11 method 1	0	+23	-23
	Ref. 7 method 1	0	+33	-33

The systematic errors are low (~ 10%), and in particular the results are not affected by the position of the jet in the transverse plane. The observation of neutral (gluon) and non-neutral (u, $\bar{u}$ quark) jets is clearly established.

6. CONCLUSION

We have presented new results on the fragmentation properties of jets in UA1. The major improvement with respect to already published data is due to the introduction of energy corrections on the measurement of jet energy, together with a very large increase in statistics. The inclusive fragmentation function is not compatible with the PETRA results, but both the fragmentation function and the internal p_T are well described by preliminary predictions based on parton showering and LUND hadronization.

A new feature is the emergence of gluon/quark differences in the fragmentation: compared with quark jets, gluon jets appear to exhibit

- higher multiplicity (low z),
- larger internal p_T,
- no charge.

The Q^2 evolution of both gluon and quark jets is coherent with QCD expectations.

Acknowledgements

I am very grateful to Professor Carlo Rubbia and to my colleagues of the UA1 experiment who made this analysis possible.

The help of Dr. Gunnar Ingelman (TH Division, CERN) with the theoretical predictions presented here is greatly appreciated.

I would also like to express my thanks to the organizers for inviting me to this Workshop.

REFERENCES

1. Banner, M. et al., Phys. Lett. 118B (1982) 203.
   Arnison, G. et al., Phys. Lett. 123B (1983) 115.

2. Horgan, R. and Jacob, M., Nucl. Phys. B179 (1981) 441.

3. Arnison, G. et al., Phys. Lett. 132B (1983) 214.

4. Buckley, E. and Kozanecki, W., CERN UA1 Technical Note, TN-85-08 (1985).

5. Arnison, G. et al., Phys. Lett. 132B (1983) 223.

6. Althoff, K. et al., TASSO Collaboration, DESY 83-130 (1983).

7. Ingelman, G., private communication.

8. Eichten, E. et al., Rev. Mod. Phys. 56 (1984) 579.

9. Combridge, B.L. et al., Phys. Lett. 70B (1977) 234.

10. Arnison, G. et al., Phys. Lett. 136B (1984) 294.

11. Field, R.D. and Feynman, R.P., Nucl. Phys. B136 (1978) 1.

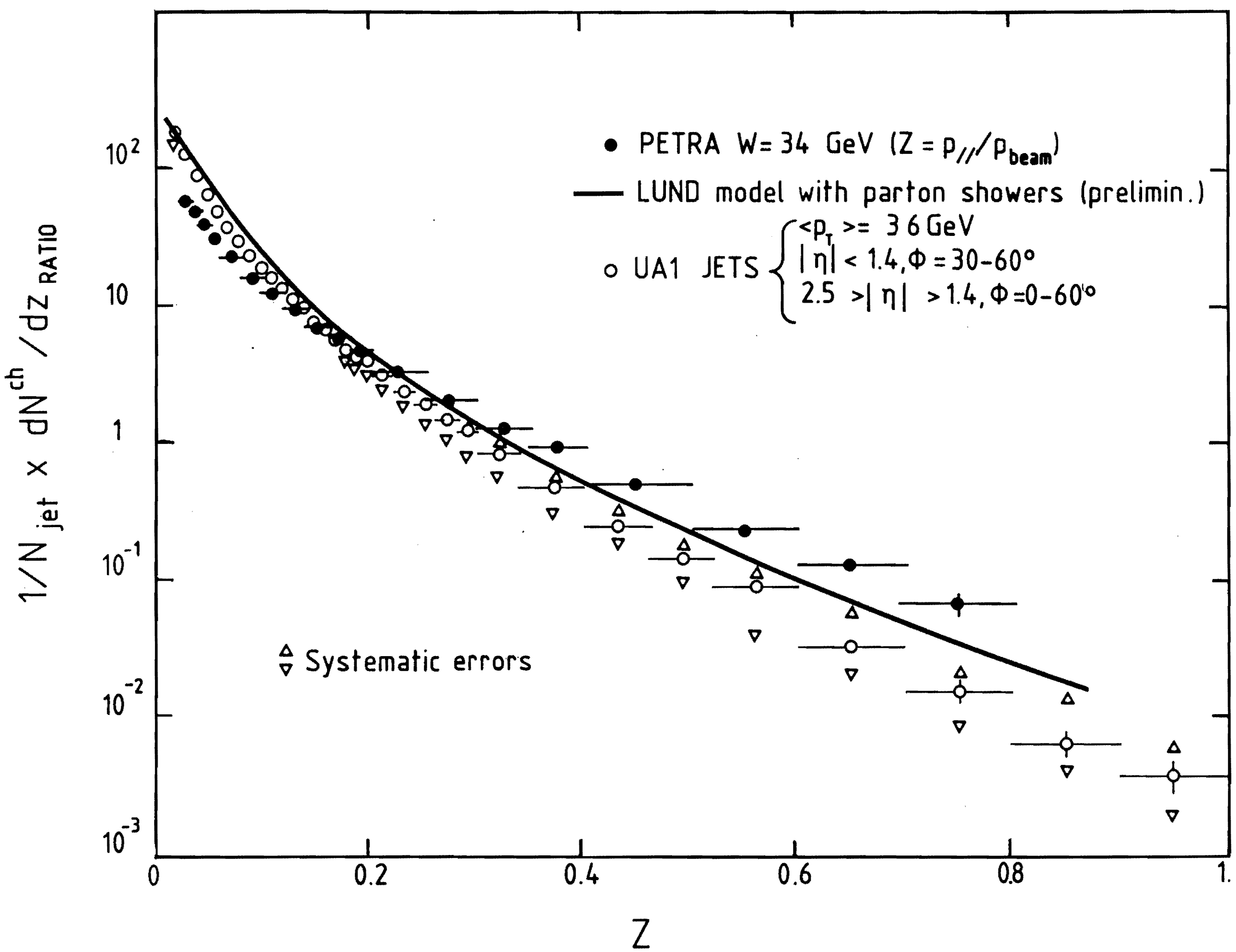

Fig. 1 Inclusive fragmentation function compared with PETRA data (Ref. 6) and the model of Ref. 7.

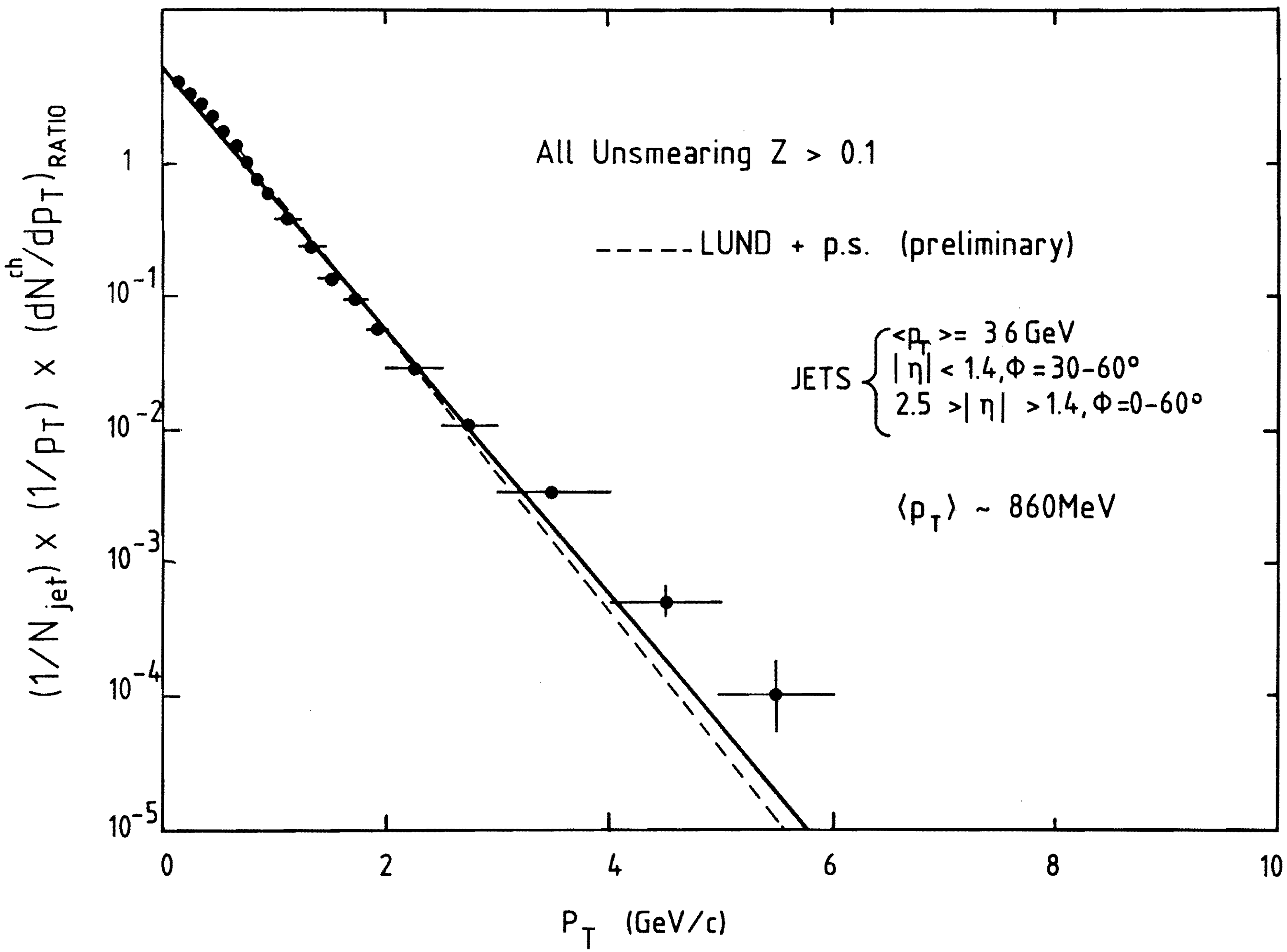

Fig. 2 Internal p_T distribution compared with the model of Ref. 7.

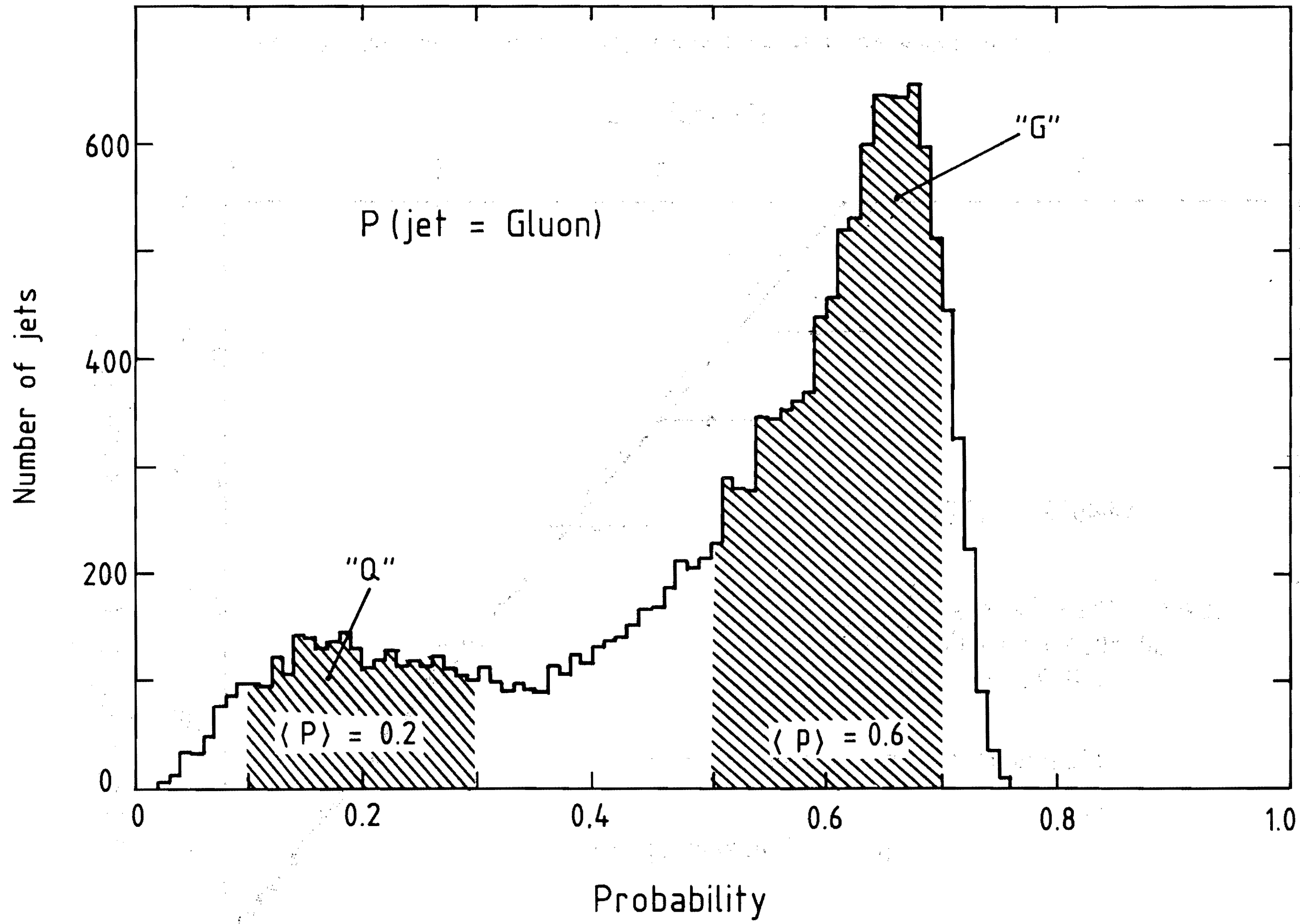

Fig. 3 Inclusive probability for a jet to be a gluon jet (see text).

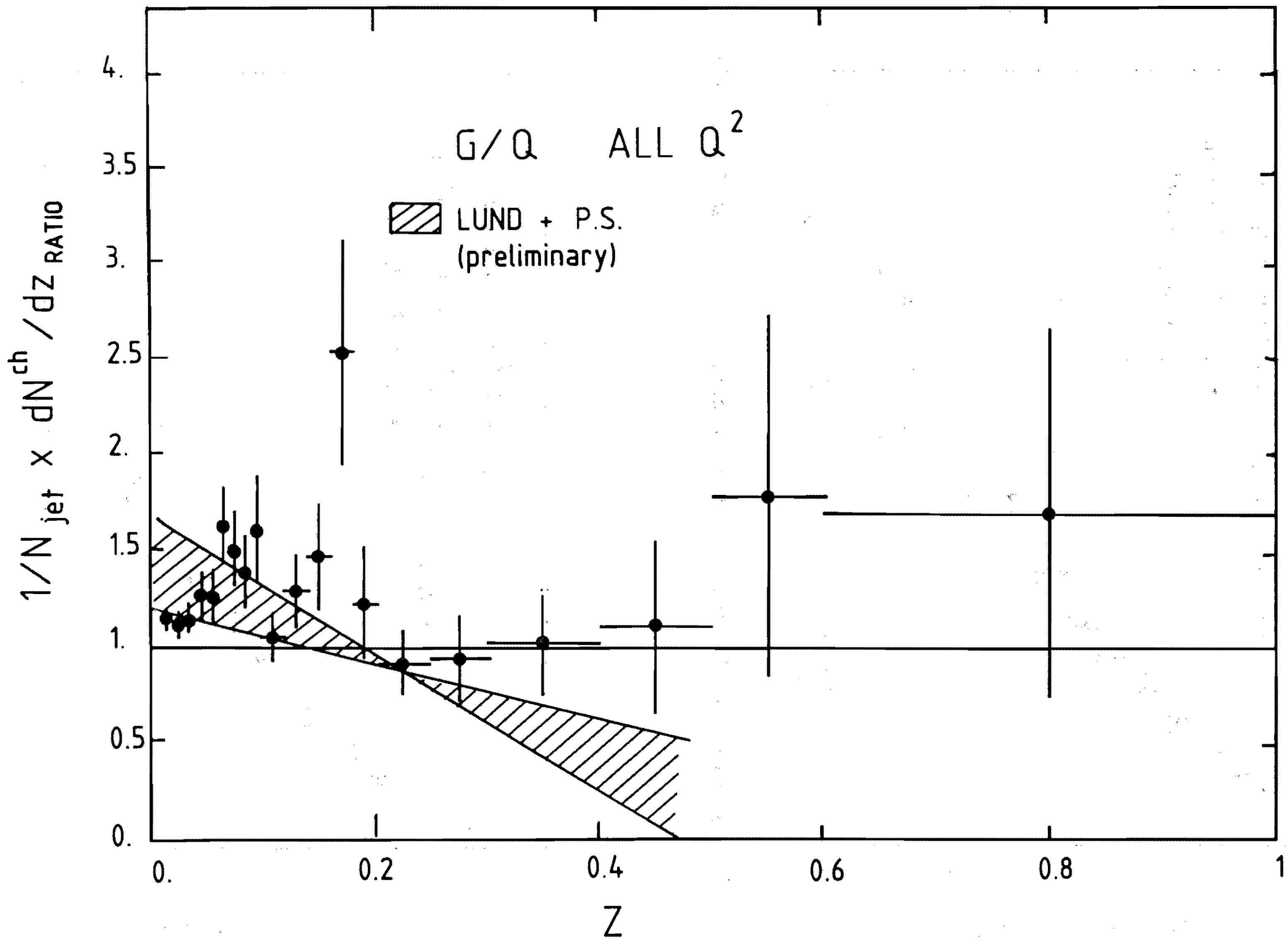

Fig. 4 Ratio between 'pure' gluon and quark fragmentation functions, compared with the model of Ref. 7.

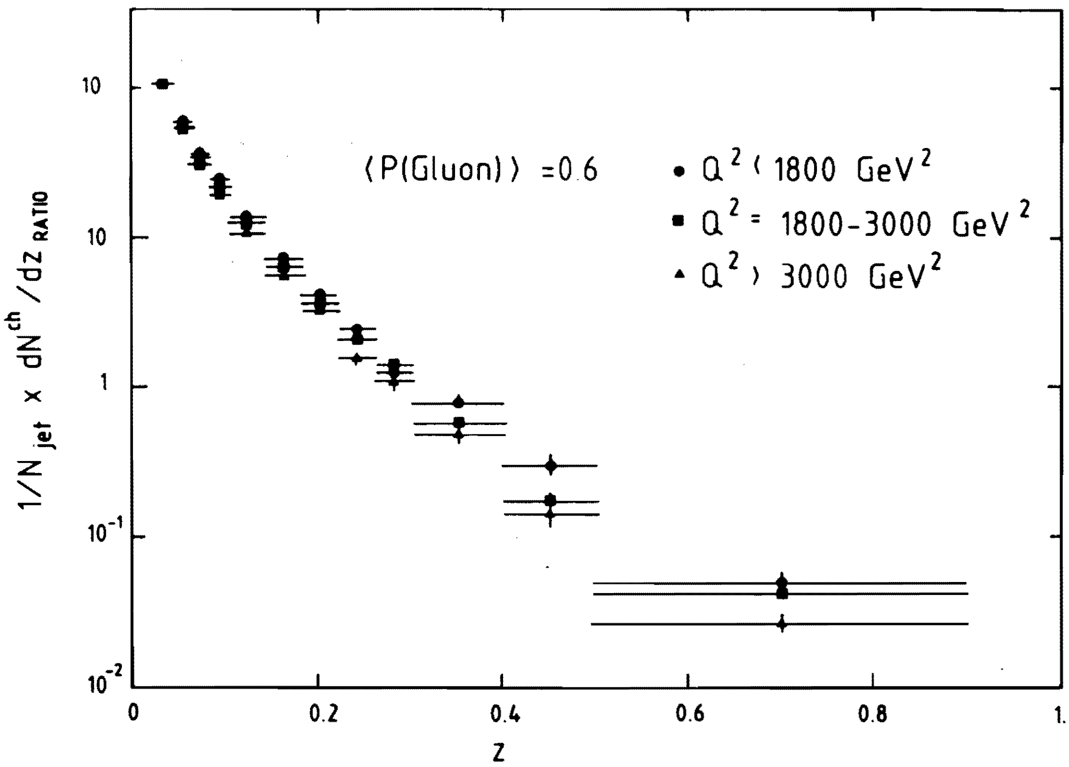

Fig. 5 Q^2 evolution of the fragmentation function for a sample enriched in gluons.

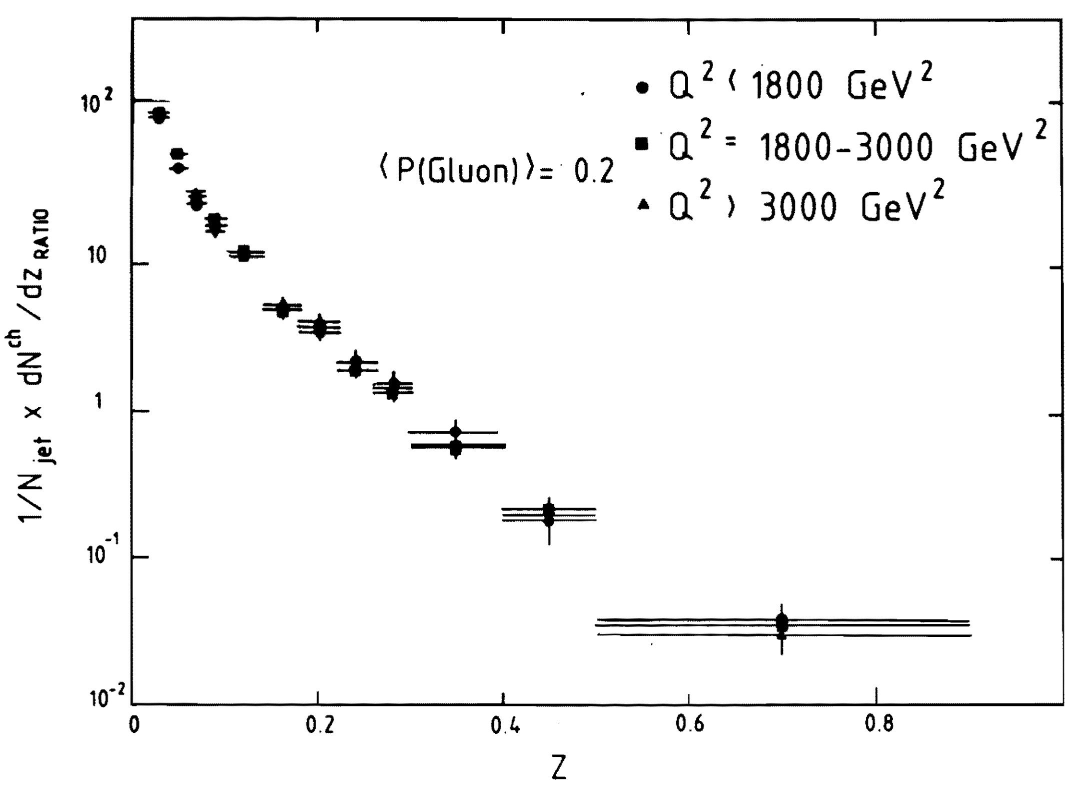

Fig. 6 Q^2 evolution of the fragmentation function for a sample enriched in quarks.

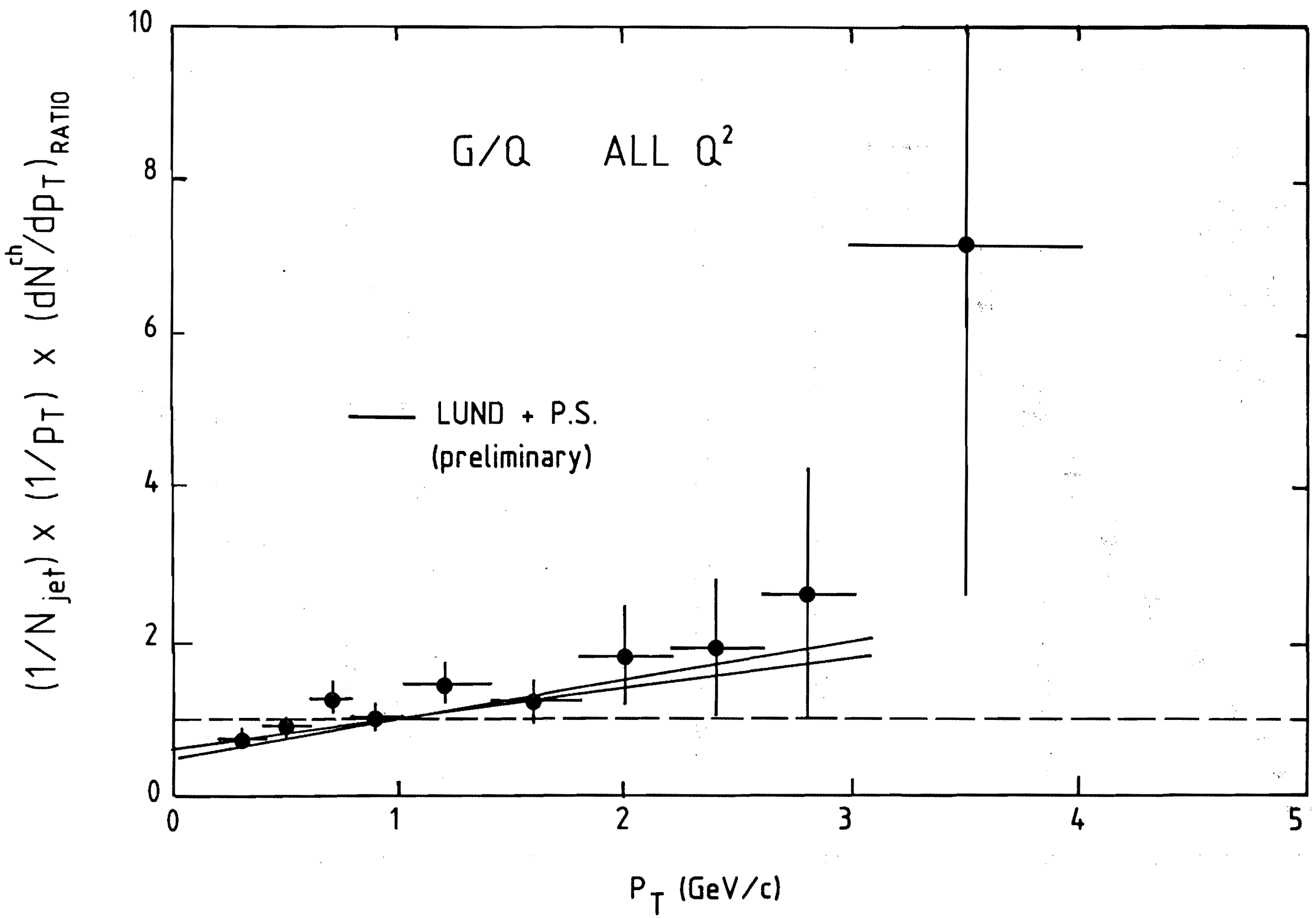

Fig. 7 Ratio between 'pure' gluon and quark internal p_T distributions, compared with the model of Ref. 7.

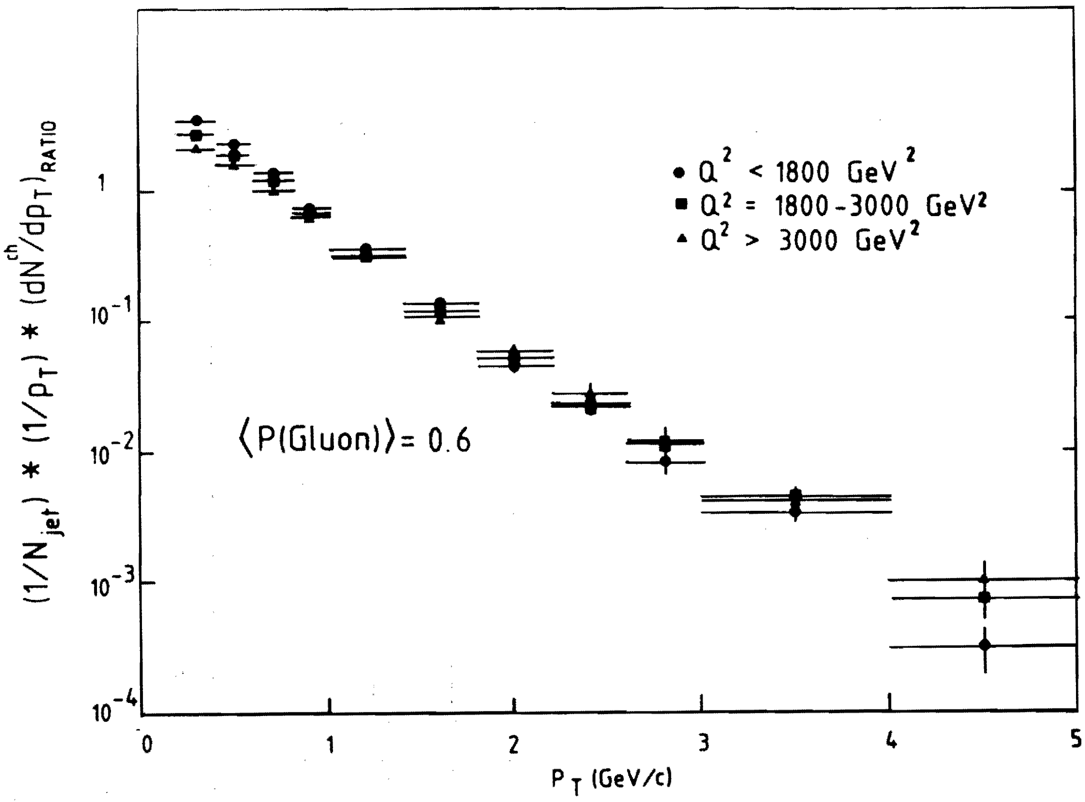

Fig. 8 Q^2 evolution of internal p_T distribution for a sample enriched in gluons.

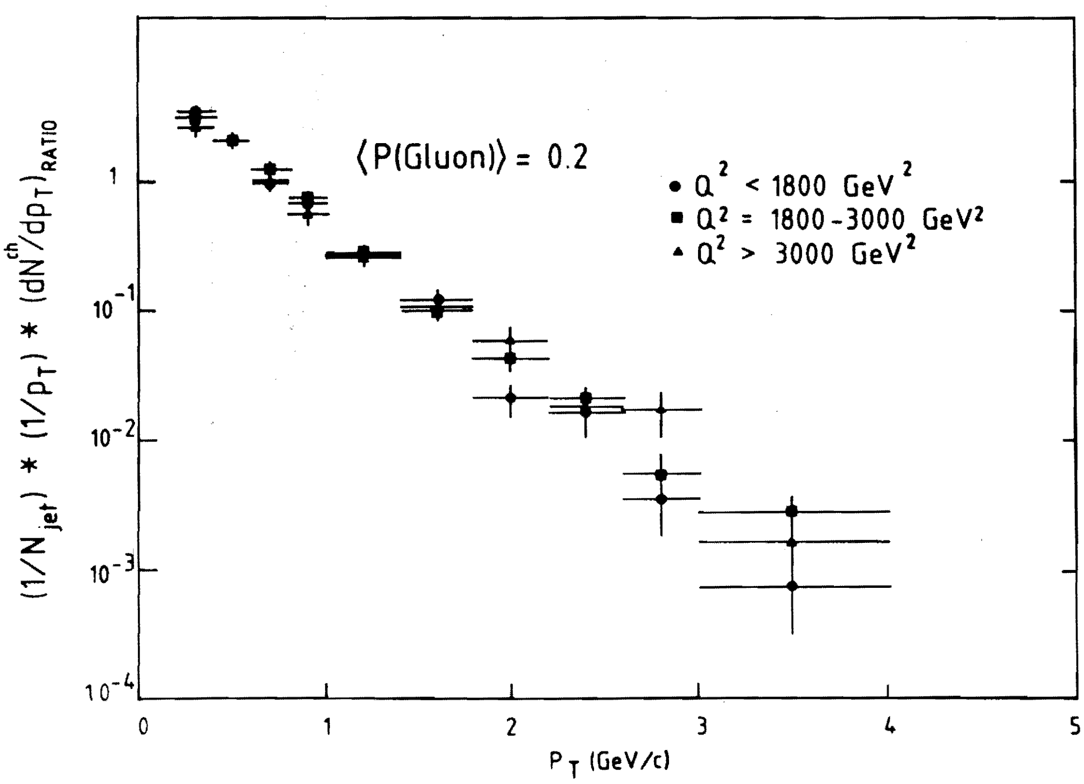

Fig. 9 Q^2 evolution of internal p_T distribution for a sample enriched in quarks.